Chapter 7
Measurements of SEPs

Abstract Those who study solar energetic particles (SEPs) should be aware of the basic types of experiments that have contributed most of the observations studied in this book, and especially the tradeoff of their strengths and weaknesses, and how they fail. However, this is *not* a comprehensive review, only an introduction. We focus on generic dE/dx versus E instruments that are the workhorses of SEP studies, and also study time-of-flight versus E instruments that dominate precision measurements below 1 MeV amu^{-1}. Single-detector instruments and high-energy techniques are discussed briefly.

Nearly every experimenter who builds instruments thinks he has made the best tradeoff within the triple constraints of weight, power, and expense, to maximize the scientific return. Many instruments are designed to extend coverage to a previously unmeasured region: energy coverage, isotope resolution, heavy elements. Others hitchhike on spacecraft going to a new and interesting region of space.

The rate of energy loss of an ion in a detector material is approximately

$$\frac{dE}{dx} \approx \frac{4\pi e^2 n_e}{mc^2\beta^2}\left(\frac{Q^2}{A}\right)\left[\ln\left(\frac{2mc^2\beta^2\gamma^2}{I}\right) - \beta^2\right] \tag{7.1}$$

where m and e are the mass and charge of an electron, n_e is the electron density, I is the "mean ionization potential" of the stopping material, and β and γ are the relativistic velocity and Lorentz factor of the ion as defined in Sect. 1.5.4. Here we have again used $E = \mathcal{E}/A = M_u\,(\gamma - 1) \approx \frac{1}{2}\,M_u\,\beta^2$, a function of velocity alone, to show that the only dependence on the stopping ion is Q^2/A and its velocity β. $M_u = m_u c^2 = 931.494$ MeV.

Equation 7.1 is derived from the electron-ion scattering cross section (Rutherford scattering) where we view incoming electrons of the stopping material being scattered by the electric field of the ion. Energy transfers to the electrons are integrated from a minimum of I to a maximum of $2mc^2\beta^2\,\gamma^2$, which is approximately the maximum energy that can be transferred to a scattered electron. Note

D.V. Reames, *Solar Energetic Particles*, Lecture Notes in Physics 932,
DOI 10.1007/978-3-319-50871-9_7

that, when $Q \approx Z$, the dominant energy dependence of dE/dx is $\sim\beta^{-2}$, or nonrelativistically, $\sim E^{-1}$, sometimes a useful approximation.

At relativistic energies, dE/dx reaches a broad minimum at ~2.5 GeV amu^{-1} then rises slightly from density effects not included here. At low energies, dE/dx actually peaks, because Q decreases, but $Q \rightarrow Z$ at moderate energies. A simple approximation sometimes used for this is $Q \approx Z\,[1–\exp(-\beta/\beta_0)]$. For capture into the K orbital, $\beta_0 \approx Z/137$; for the Fermi-Thomas model $\beta_0 \approx Z^{2/3}/137$. Modern empirical tables use more complex expressions and tabulate both stopping power and range (Hubert et al. 1990). The particle range $R = \int dE\,(dE/dx)^{-1}$. For energies down to 1 keV amu^{-1}, the tables of Paul and Schinner (2003) are available.

7.1 Single-Element Detectors

Conceptually, the simplest detector is that with a single sensitive element. Modern "solid-state" detectors are a Si wafer biased as a capacitor that collects the electron-hole pairs produced when an ionizing particle penetrates, loses energy, or stops within its volume. The charge collected, proportional to the energy loss, is measured as a pulse height by analog-to-digital converters. Single-element detectors are generally shielded to define the access geometry for low-energy particles.

Measuring the energy of each arriving particle works at low energies, but penetrating particles contribute as if they had a much lower energy (Fig. 7.1).

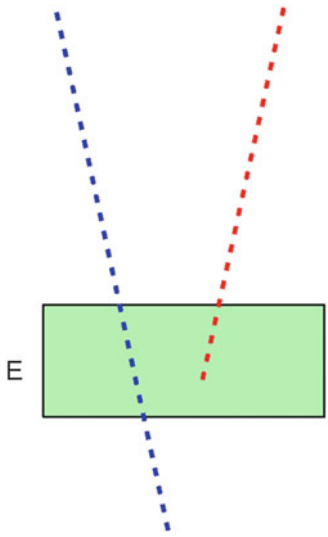

Fig. 7.1 A single-detector telescope measures the total kinetic energy of stopping ions (*red*) and the energy loss of penetrating ions (*blue*), which is much lower. The latter are (incorrectly) assumed to be rare. Access geometry is somewhat controlled by shielding (not shown) and a permanent magnet may be included to sweep away electrons, or to measure electrons by comparing detectors with and without magnets

When the SEPs have a steep energy spectrum, the contribution of high-energy particles may be small, but early in SEP events nearly all particles are penetrating and single-detector instruments falsely appear to show low-energy particles arriving much earlier than they possibly could. This effect is sometimes called "punchthrough," it occurs in *every* SEP event, and can cause serious misconceptions. These detectors also confuse heavier ions similarly, even though they deposit an increasing amount of energy. Single-element telescopes should never be used for SEP onset timing. They are more appropriate for the study of energetic particle spectra at interplanetary shock waves.

Electrons are particularly difficult to measure since they do not travel in straight lines, but suffer numerous large-angle scatters. The best remedy is extensive instrument calibration before launch.

Single-element and other limited telescopes are sometimes flown on deep-space missions where weight and power are severely limited and where SEPs are not the primary objective. Unfortunately, these low-priority hitchhikers may even be turned off during transit to the mission destination to save resources, greatly decreasing their value.

7.2 ΔE Versus E Telescopes

These telescopes consist of at least three active detector elements. Particles enter the first detector, penetrate into the second, and stop before entering the third anti-coincidence detector. The separation of the first two detectors, and their areas, determine the instrument geometry-factor. The detector thicknesses determine the minimum and maximum energy according to the range-energy relation in Si (e.g. Hubert et al. 1990). Front detector thicknesses of 10–20 μm set a lower bound of ~1 MeV amu^{-1}, depending upon species. Total thicknesses of D + E of up to 10 cm of Si are used for energies ~200 MeV amu^{-1}. The energy range can be extended to above ~400 MeV amu^{-1} by observing the *change* in dE/dx between D and E, if penetrating ions are measured. The concept of a two-element telescope is shown in Fig. 7.2.

Most of the particle telescopes flown in space are of this general type, although multiple detectors may be used in place of the D and E elements. Early telescopes used plastic scintillator or even gas drift chambers, but most telescopes of the last 20 years are "solid state" Si detectors which have extremely high resolution and *stability*, i.e. *their response does not change at all during several decades of operation*.

Anti-coincidence detectors were sometimes wrapped around the whole telescope. However, at the high rates in a large SEP event these may be recording particles nearly all the time, and insure that the telescope is effectively turned off.

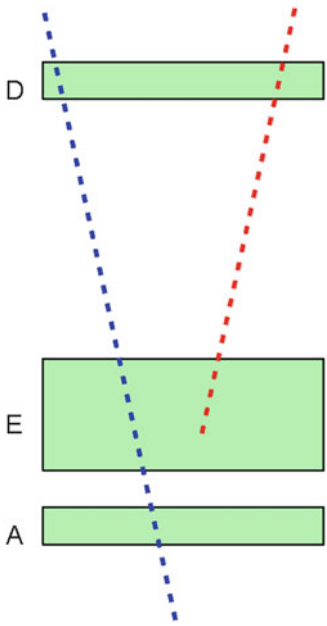

Fig. 7.2 A minimal ΔE versus E or two-dimensional telescope requires coincidence of signals from the D and E elements and no signal from the A element to define stopping (*red*) ions. "Matrix" plots of pulse-heights of D versus E are used to resolve elements and measure their energies (see Fig. 7.3). The anti-coincidence element or inert shielding may surround the telescope

A geometry factor defined by surfaces S_1 and S_2 is

$$A\Omega = \iint_{S_1} dS_1 \iint_{S_2} dS_2 \frac{(\mathbf{n}_1 \cdot \mathbf{r})(\mathbf{n}_2 \cdot \mathbf{r})}{r^4} \tag{7.2}$$

where $\boldsymbol{n}_1$ and $\boldsymbol{n}_2$ are unit vectors normal to the surface elements dS_1 and dS_2, respectively and $\boldsymbol{r}$ is the vector distance between them. Geometry factors are usually calculated numerically.

7.2.1 An Example: LEMT

Response of a telescope with a thin front detector, the *Low-Energy Matrix Telescope* (LEMT) on the *Wind* spacecraft (von Rosenvinge et al. 1995), is shown in Fig. 7.3. LEMT has three important virtues, large geometry (51 cm^2 sr), broad element

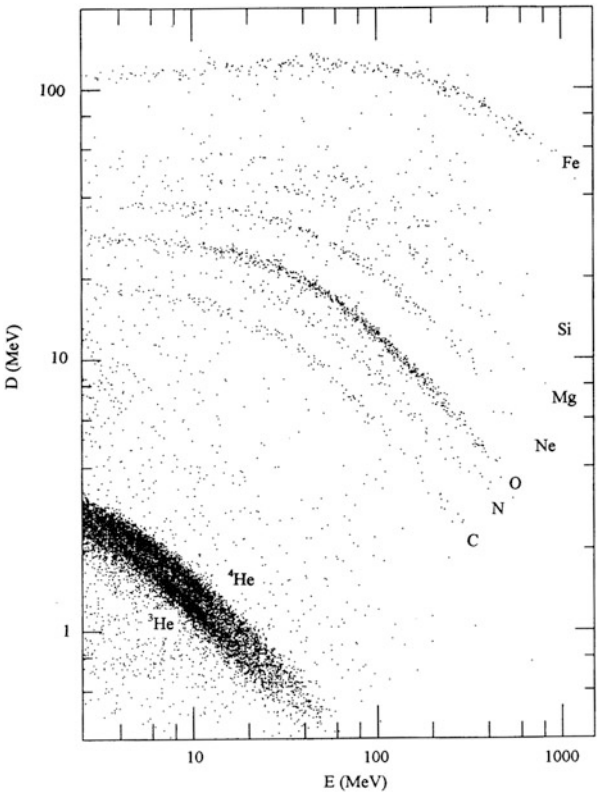

Fig. 7.3 Response of the LEMT telescope to ions from a small ^{3}He-rich event in 1995 is shown with "tracks" of species indicated. The telescope has only modest resolution of He isotopes. The track of O is heavily populated by anomalous cosmic rays during this period near solar minimum (see Reames et al. 1997)

coverage (He–Pb at ~2–20 MeV amu^{-1}), and, equally important, the author is familiar with it. Each LEMT consists of a domed array of 16 D-detectors 18 μm thick, followed by a large 1-mm-thick E-detector with coarse 5 × 5 position sensing and an anticoincidence detector (see von Rosenvinge et al. 1995).

Particles entering LEMT are corrected for angle of entry, mapped in a log D versus log E space, like that of Fig. 7.3, and binned onboard according to particle species and energy interval (see Reames et al. 2001). The right-hand ends of the particle tracks, especially noticeable for C, N, and O, occur just before the ions have enough energy to begin to penetrate into the anticoincidence detector.

In the region of the rarer elements with $Z \geq 34$, "priority" measurements of individual ions are rare enough to be telemetered for later analysis. The performance of LEMT at high Z is shown in Fig. 7.4.

While the error at high Z is 2–3 units, the resolution is adequate to show bands of enhanced abundances, such as that between Ge and Zr and the band near Sn, that reflect an abundance maximum at $50 \leq Z \leq 56$. The absolute locations of the reference curves of the elements were calibrated prior to launch using accelerator

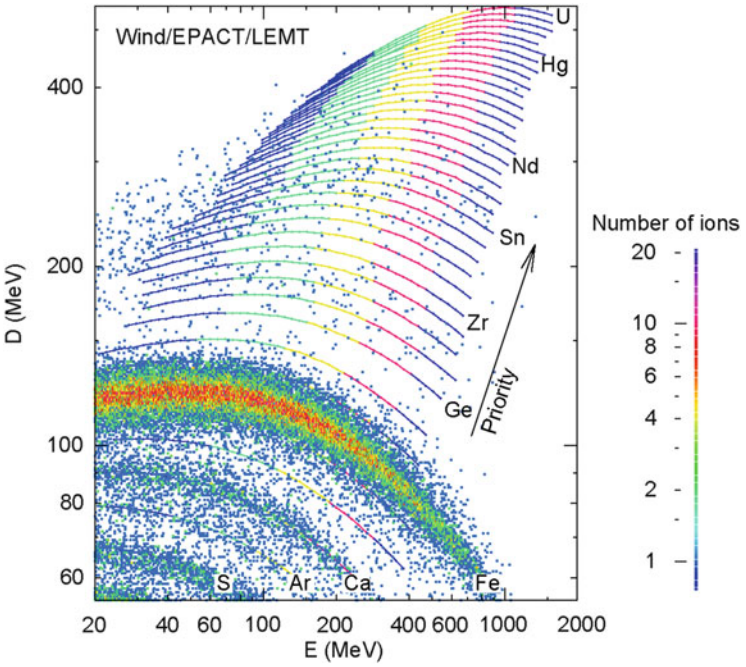

Fig. 7.4 High-Z response of LEMT is shown where resolution (i.e. track width) is comparable with that at Fe. Energy varies along each calibration curve from *left* to *right*, from 2.5 to 10 MeV amu^{-1}

beams of He, C, O, Fe, Ag, and Au (see von Rosenvinge et al. 1995). By measuring at low energy with a fairly large geometry factor, LEMT can move up the steep energy spectra to get a rough measure of the abundances of the rare elements with $34 \leq Z \leq 82$. For results of these measurements see Figs. 4.7 and 4.9.

7.2.2 *Isotope Resolution: SIS*

Accuracy can be affected by thickness variations and sec θ variations by particle trajectories inclined by an angle θ to the telescope axis. Both of these may be reduced by accurately measuring sec θ using two sets of x and y strip detectors (e.g. Stone et al. 1998). The additional detector thickness required for these measurements raises the energy threshold above ~10 MeV amu^{-1}, depending upon particle species, but also permits isotope resolution up to Fe—an important tradeoff. Figure 7.5 shows the resolution of Ne isotopes by the *Solar Isotope Spectrometer* (SIS) on the *Advanced Composition Explorer* (ACE) in two different SEP events. Isotopic abundances show the same A/Q variations we have seen in

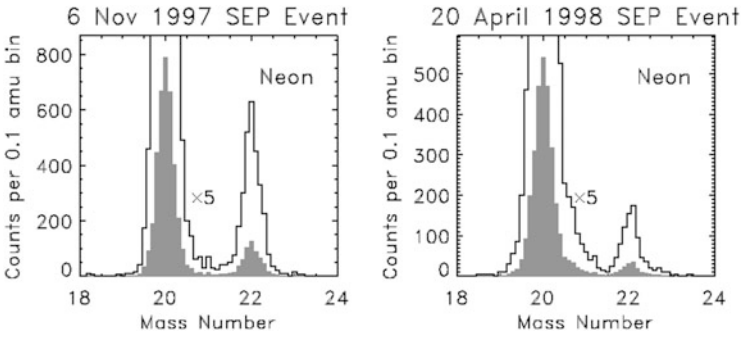

Fig. 7.5 Panels show the resolution of Ne isotopes by the SIS telescope in two SEP events. Histograms are also shown enhanced by a factor of 5 to clarify ^{22}Ne measurement (Leske et al. 2007). Isotope measurements show A/Q enhancements like those seen in element abundances

element abundance enhancements in both impulsive and gradual SEP events. Here, however, there is no question about the average value of Q, which we expect to be the same for all isotopes of an element.

7.3 Time-of-Flight Versus E

Measurement of a particle's time of flight over a fixed distance determines its velocity. If the particle subsequently stops in a Si detector its total kinetic energy can be measured, and the pair of measurements determines the particle mass. The design of the *SupraThermal Energetic Particle* (STEP) system flown on the *Wind* and STEREO spacecraft is shown in Fig. 7.6.

A particle penetrating the entrance Ni foil in STEP may knock off ~4–30 electrons that are accelerated and deflected by the 1 kV electric field into the "start" microchannel plates that multiply the signal by ~100. If the particle then enters the Si detector, backscattered electrons are accelerated into the "stop" microchannel plates, and energy is measured in the Si detector. The time between the start and stop signals, 2–100 ns, is processed by a time-to-amplitude converter (TAC). The TAC and energy signals are combined into a weighted analog sum that assigns a priority that controls further processing. Heavies, with $A > 4$, are assigned the highest priority, He next, and then H.

The response of STEP to a small ^{3}He-rich SEP is shown in Fig. 7.7.

The resolution using this technique can be greatly improved by adding an additional timing plane, using electrostatic mirrors to reflect the electrons, and using microchannel plates with position-sensing anodes. This was done for the ULEIS instrument on the ACE spacecraft (Mason et al. 1998). This instrument produced the resolution seen in Fig. 4.16.

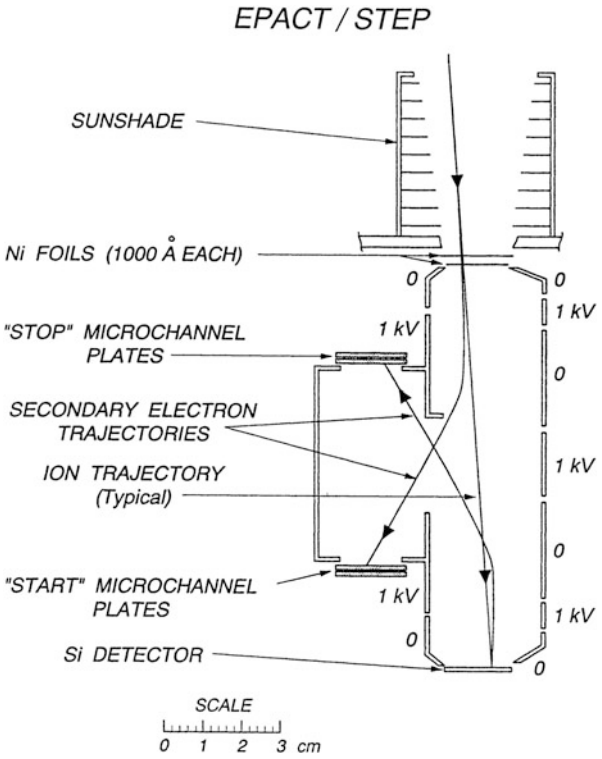

Fig. 7.6 The STEP telescope measures time of flight versus energy (see text; von Rosenvinge et al. 1995)

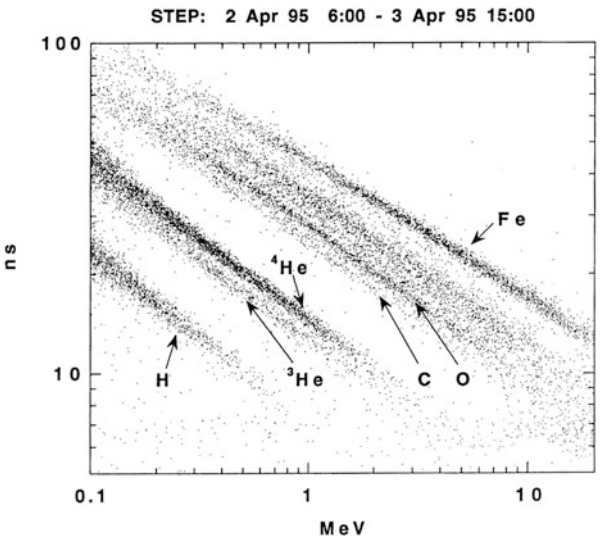

Fig. 7.7 The response of the STEP telescope shows the time-of-flight (ns) versus the total kinetic energy (MeV) for a sample of ions during a small ^{3}He-rich SEP event (see von Rosenvinge et al. 1995; Reames et al. 1997)

7.4 NOAA/GOES

The *Geostationary Operational Environmental Satellites* (GOES), operated by the *National Oceanic and Atmospheric Administration* (NOAA), are a series of satellites intended to give continuous time coverage of the space environment. A new GOES spacecraft with equivalent capabilities is launched every few years.

Energies of interest for SEP observations are proton energies in five channels from 4 to 500 MeV measured by two-element telescopes behind different thicknesses of shielding in the *Energetic Particle Sensor* (EPS). In addition, the *High Energy Proton and Alpha Detector* (HEPAD) adds a Cherenkov detector to measure protons in the intervals 350–420, 420–510, 510–700, and >700 MeV. These are extremely useful high-energy measurements. GOES data since 1986 are available at http://satdat.ngdc.noaa.gov/sem/goes/data/new_avg/ (although the web site has been known to change). Note that the low-energy channels of the EPS should *not* be used for onset timing since they are contaminated by higher-energy particles. Geometry factors for high-energy particles are too uncertain to allow channel differences to exclude all contamination in EPS. However, GOES provides an excellent synoptic summary of SEP events (see Fig. 5.1) and the >700 MeV channel may be a better indicator of a high-energy protons than neutron monitors (Thakur et al. 2016).

GOES also provides 1–8 Å soft X-ray peak intensities that is a classic measure of heating in solar flares. The X-ray "CMX class" specifies the decade of X-ray peak intensity with Cn for $n \times 10^{-6}$ W m^{-2}, Mn for $n \times 10^{-5}$ W m^{-2}, and Xn for $n \times 10^{-4}$ W m^{-2} (e.g. see Fig. 4.13).

7.5 High-Energy Measurements

Ground-level neutron monitors have provided the historic information on SEPs above ~0.5 GeV by observing the products that rain down from nuclear interactions of energetic protons with atomic nuclei of the upper atmosphere. When the signal from the SEPs can be seen above the background produced by galactic cosmic rays we have a ground-level event (GLE). However, many GLEs rise less than 10% above background, providing rather poor information on timing.

As noted previously, high-energy protons are often strongly beamed along the interplanetary magnetic-field line, so a particular neutron monitor on Earth sees an intensity maximum when its asymptotic look direction is aligned with that field. Since the field direction can vary, neutron monitors often see sudden increases or decreases, or even multiple peaks and valleys of intensity as their look direction scans across the pitch-angle distribution as the interplanetary magnetic-field direction swings around. Nevertheless, integrating over an event at multiple stations can produce creditable spectra, that compare well with those from GOES and IMP, as

obtained by Tylka and Dietrich (2009) and shown in Figs. 6.2 and 6.3. This was a significant advance in high-energy spectra.

Two newer instruments, the *Payload for Antimatter Exploration and Light-nuclei Astrophysics* (PAMELA) mission and the *Alpha Magnetic Spectrometer* (AMS) are large complex instruments that were justified and funded for particle physics and cosmology, which may also prove useful for high-energy SEP measurements. These instruments use transition-radiation detectors, time-of-flight detectors, a permanent magnet and tracking system, Cherenkov systems, and calorimeters to measure each incident particle. They were designed to search for antimatter, such as anti-helium, strange quark matter, and dark matter.

The PAMELA satellite is in a near-polar, 70°–inclination, orbit. It can measure protons and He above about 80 MeV amu^{-1} and reported spectra for the 13 December 2006 SEP event (Adriani et al. 2011) and for several events in 2010–2012 (Bazilevskaya et al. 2013). AMS is on the *International Space Station*. It can measure protons and isotopes of light ions above about 200 MeV amu^{-1}.

While these instruments must deal with geomagnetic-field limitations, as neutron monitors do, they can directly measure spectra and abundances and represent a great improvement in the accuracy of measurements at high energies.

7.6 Problems and Errors

The single most difficult problem in measuring SEPs is exploring rare species and small events while still dealing with the high intensities in large events. Most high-resolution instruments fail or degrade during periods of *high SEP intensity*.

Early instruments sampled particles randomly and sent the measurements to the ground for analysis. However, since telemetry was slow and the H/O ratio can exceed 10^4 at fairly high energies, H and He consumed all the telemetry and heavy ions were almost never seen. Later instruments incorporated priority schemes to distinguish H, He, and "heavies" and selectively telemetered them at different priorities, keeping track of the number received onboard for re-normalization. Most modern instruments determine particle species and energy and bin them onboard in most cases. The higher onboard processing rates have allowed geometry factors to profitably expand, improving statistics and observing rare species.

As rates increase, the first problem to solve involves "dead-time corrections." An instrument cannot process a new particle while it is still busy processing the previous one. Knowing the processing times, these corrections are usually already made while calculating intensities. However, it does make a difference whether the telescope has become busy because too many high-energy particles traverse the anticoincidence detector, or because too many low-energy particles are striking the front detector. Some instruments can determine coincidence and priority at high rates before they decide to perform the slower pulse-height analysis; they can handle much higher throughput. Instruments that must pulse-height analyze every above-threshold signal in every detector are more limited in

speed, by factors of 10 or more, since many of the pulse heights are not of interest; perhaps they do not even meet the coincidence conditions.

Eventually, problems come from multiple particles in the telescope within the resolution time. A proton stops in the back detector and triggers the coincidence while a low energy Fe stops in the front detector, or while an energetic He or heavier ion crosses the front detector at some large angle. Background in LEMT during the first day of the Bastille-Day SEP event on 14 July 2000 is shown in Fig. 7.8. Background stretches all the way up the ordinate in the $2 < E < 20$ MeV band. Calibration curves that are shown have omitted the 2.5–3.3 MeV amu^{-1} interval which would extend into this band. The added background not only contaminates measurements but also reduces the time available for real particles. Fortunately this is a rare problem for LEMT and it fails quite gracefully in this case, i.e. abundances and spectra above 3.3 MeV amu^{-1} are still quite useful.

The upper limit of E of the background band in LEMT occurs because it is difficult for a proton, the most abundant species, to deposit more than 10 or 15 MeV into the E detector before penetrating into the anticoincidence detector.

One easy way to detect background is to check for unrealistic abundances, such as measurable ratios F/O or B/O. *If you discover something really unusual, it is wise to check the pulse-height matrix before publishing your new finding.*

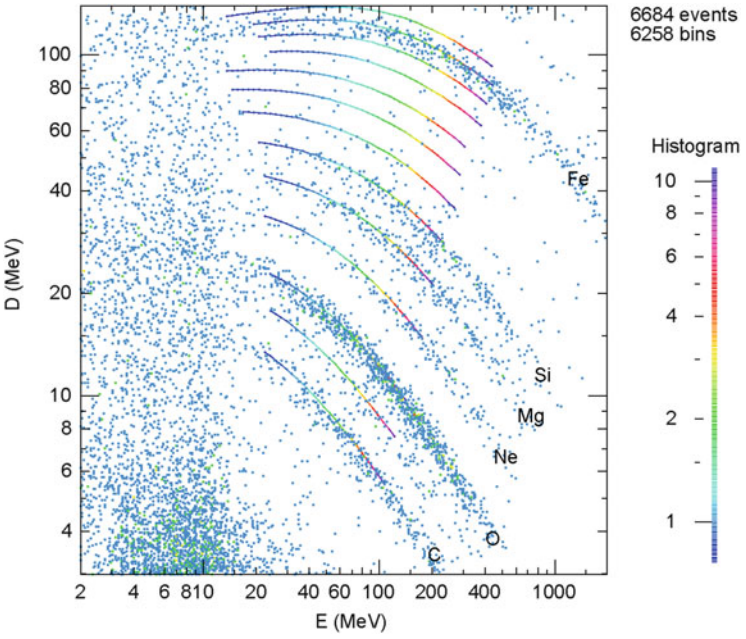

Fig. 7.8 Sampled response of LEMT is shown during the first day of the Bastille-Day event, 14 July 2000. Calibration curves are only shown from 3.3–10 MeV amu^{-1}, to emphasize the band of background covering the region where the 2.5–3.3 MeV amu^{-1} interval would be. Compare the region $2 < E < 20$ MeV with that in Fig. 7.3

Different instruments have different problems and some have interesting solutions. Some early instruments suffered gain changes in large events so the particle tracks moved around with time. *Many* instruments saturate at high particle rates, the smaller, faster instruments on GOES and *Helios* do not. ULEIS has a restricting aperture that can be rotated into place to reduce intensities. Other telescopes turn off detector elements to reduce their geometry factor.

The data base for many measurements from many spacecraft, including SEP intensities, is http://cdaweb.gsfc.nasa.gov/sp_phys/. Generally, however, pulse-height data are not widely available, since the more-extensive data and specialized processing and software required are only developed by the instrument teams. This software is generally not modified to keep up with evolution of computer hardware and operating systems.

References

Adriani, O., Barbarino, G.C., Bazilevskaya, G.A., Bellotti, R., Boezio, M., Bogomolov, E.A., Bonechi, L., Bongi, M., Bonvicini, V., Borisov, S., et al.: Observations of the 2006 December 13 and 14 solar particle events in the 80 MeV n^{-1}–3 GeV n^{-1} range from space with the PAMELA detector. Astrophys. J. **742**, 102 (2011)

Bazilevskaya, G.A., Mayorov, A.G., Malakhov, V.V., Mikhailov, V.V., Adriani, O., Barbarino, G.C., Bellotti, R., Boezio, M., Bogomolov, E.A., Bonechi, L., et al.: Solar energetic particle events in 2006–2012 in the PAMELA experiment data. J. Phys. Conf. Ser. **409**, 012188 (2013). doi:10.1088/1742-6596/409/1/012188

Hubert, F., Bimbot, R., Gauvin, H.: Range and stopping-power tables for 2.5–500 MeV/nucleon heavy ions in Solids. Atom. Dat. Nucl. Dat. Tables. **46**(1), (1990)

Leske, R.A., Mewaldt, R.A., Cohen, C.M.S., Cummings, A.C., Stone, E.C., Wiedenbeck, M.E., von Rosenvinge, T.T.: Solar isotopic composition as determined using solar energetic particles. Space Sci. Rev. **130**, 195 (2007)

Mason, G.M., Gold, R.E., Krimigis, S.M., Mazur, J.E., et al.: The ultra-low-energy isotope spectrometer (ULEIS) for the ACE spacecraft. Space Sci. Rev. **86**, 409 (1998)

Paul, H., Schinner, A.: Empirical stopping power tables for ions from ^{3}Li to ^{18}Ar and from 0.001 to 1000 MeV/nucleon in solids and gases. Atom. Dat. Nucl. Dat. Tables. **85**, 377 (2003)

Reames, D.V., Barbier, L.M., von Rosenvinge, T.T., Mason, G.M., Mazur, J.E., Dwyer, J.R.: Energy spectra of ions accelerated in impulsive and gradual solar events. Astrophys. J. **483**, 515 (1997)

Reames, D.V., Ng, C.K., Berdichevsky, D.: Angular distributions of solar energetic particles. Atrophys. J. **550**, 1064 (2001)

Stone, E.C., Cohen, C.M.S., Cook, W.R., Cummings, A.C., Gauld, B., Kecman, B., Leske, R.A., Mewaldt, R.A., Thayer, M.R., Dougherty, B.L., et al.: The solar isotope spectrometer for the advanced composition explorer. Space Sci. Rev. **86**, 357 (1998)

Thakur, N., Gopalswamy, N., Mäkelä, P., Akiyama, S., Yashiro, S., Xie, H.: Two exceptions in the large SEP events of solar cycles 23 and 24. Sol. Phys. **291**, 513 (2016)

Tylka, A.J., Dietrich, W.F.: A new and comprehensive analysis of proton spectra in ground-level enhanced (GLE) solar particle events. In: Proceedings of 31st International Cosmic Ray Conference, Lódz (2009). http://icrc2009.uni.lodz.pl/proc/pdf/icrc0273.pdf

von Rosenvinge, T.T., Barbier, L.M., Karsch, J., Liberman, R., Madden, M.P., Nolan, T., Reames, D.V., Ryan, L., Singh, S., Trexel, H.: The energetic particles: acceleration, composition, and transport (EPACT) investigation on the *Wind* spacecraft. Space Sci. Rev. **71**, 152 (1995)